Radiomics in oncology: present and future

Carolina de la Pinta Alonso

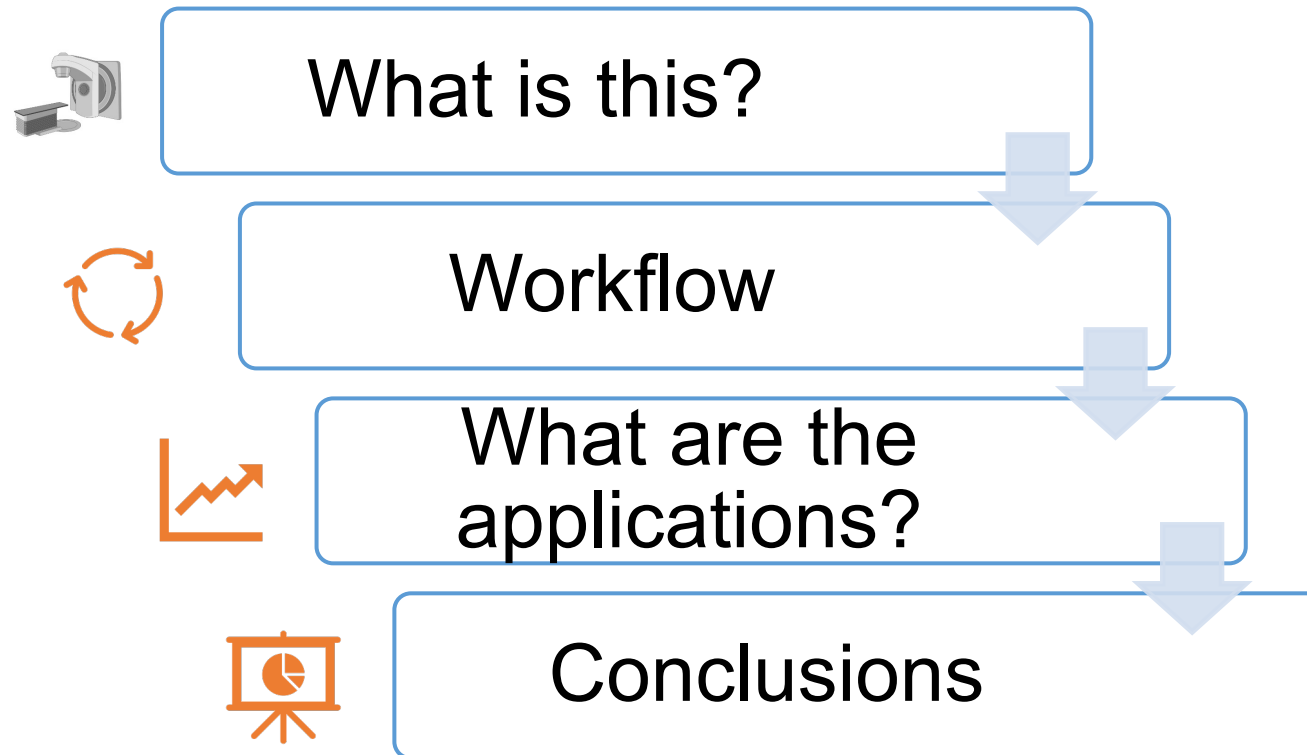Physician in radiation oncology, MD, PhD

Hospital Universitario Ramón y Cajal, Madrid, Spain

TABLE OF CONTENTS

What is this?

Workflow

What are the applications?

Conclusions

WHAT IS THIS?

RADIOMICS I

- Radiomics makes it possible to analyze and extract data from medical images, including **quantitative** and **qualitative** characteristics.

- CT, MRI and PET using computer software.

- More precise **delimitation of tumor**, the tumor **microenvironment** or alterations **after treatment**.

RADIOMICS II

This requires:

1. Image acquisition
2. Dataset creation
3. Export of DICOM studies
4. Identification of the volume of interest (VOI) using segmentation tools
5. Feature extraction and qualification
6. Study of the data
7. Construction of a predictive model
8. Validation of the created models

Kumar V, et al. Magn Reson Imaging 2012;30:1234–1248. Katabathina VS, et al. Radiographics 2020;40:1600–1626

RADIOMICS III

The use of convolutional neural networks (CNNs) in medical image analysis is growing, outperforming traditional machine learning (ML) algorithms on large datasets.

Problems

- Large variability in medical concepts

- ⬇ number of studies

Pre-training studies is proposed with promising results for different image analysis tasks.

Ziegelmayer S, et al. J Clin Med 2020;9:4013. Barat M, et al. Jpn J Radiol 2021;39:514–523. Weisberg EM, et al. Diagn Interv Imaging 2020;101:111–115. Kaissis G, et al. Eur Radiol Exp 2019;3:41.

RADIOGENOMICS

PRECISION MEDICINE

Correlation of studies between **genomics** and **molecular** measurements and **radiological** studies to be established, improving diagnosis and patient stratification.

Bartoli M, et al. Jpn J Radiol 2020;38:1111–1124.

Table 1. Short definitions for specific medical terms.

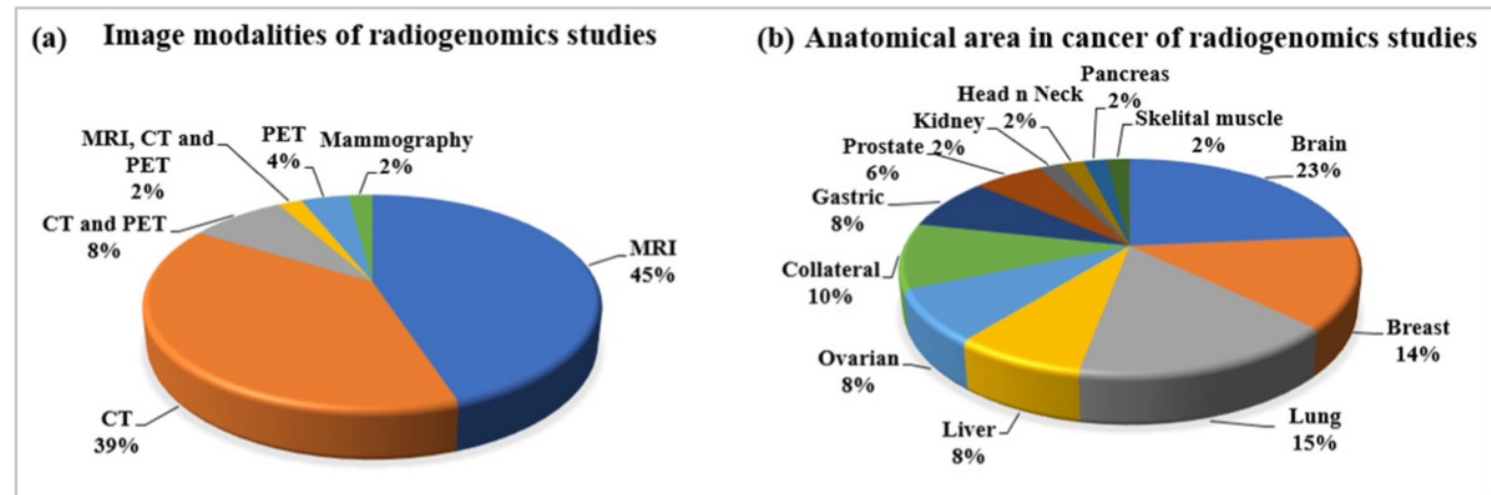| Terminology	Short Definition
Radiomics	Quantitative approach to medical imaging, enhancing existing data through mathematical analysis [68].
Genomics	Study of whole genomes, including elements from genetics. Genomics uses a combination of recombinant DNA, DNA sequencing methods, and bioinformatics to sequence, assemble, and analyze the structure and function of genomes [69–71].
Radiogenomics	Genomics information that can be explained or decoded by radiomics and to develop methodology to create more-efficient predictive models [72].

DNA = deoxyribonucleic acid.
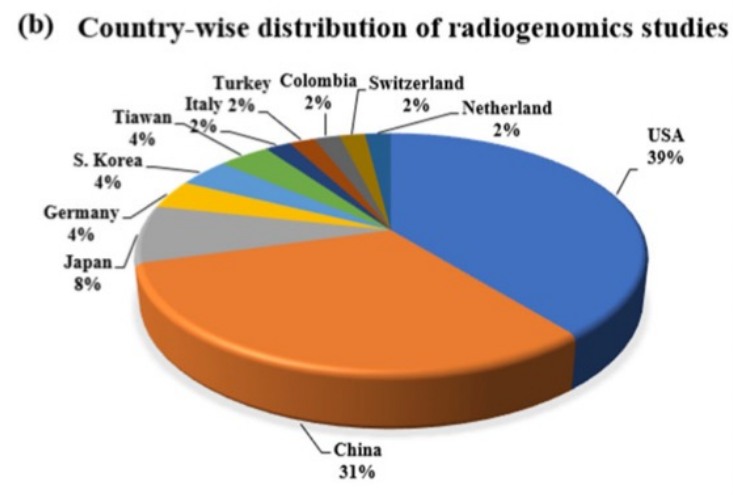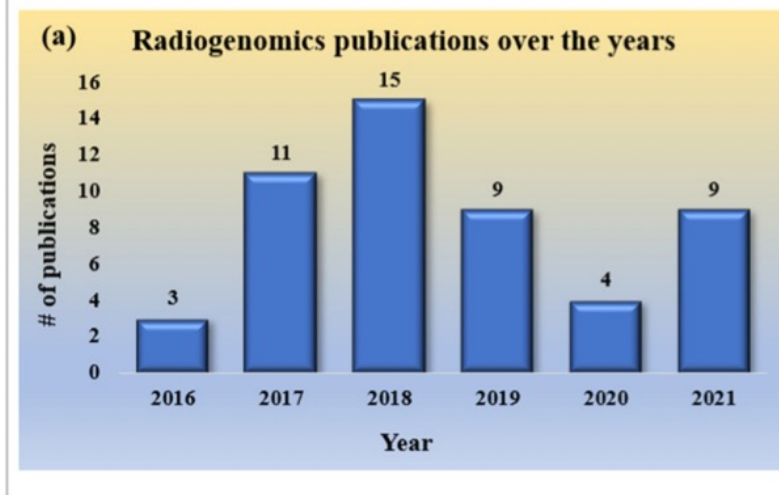
Figure 2. (**a**) Publication trends; (**b**) country-wise distribution of radiogenomics studies.

Figure 4. (**a**) Image modalities; (**b**) anatomical cancer in radiogenomics studies.

Saxena S, Jena B, Gupta N, Das S, Sarmah D, Bhattacharya P, Nath T, Paul S, Fouda MM, Kalra M, Saba L, Pareek G, Suri JS. Role of Artificial Intelligence in Radiogenomics for Cancers in the Era of Precision Medicine. Cancers (Basel). 2022 Jun 9;14(12):2860.

WORKFLOW

4-CONSTRUCTION OF MODELS

3-EXTRACTION AND QUANTIFICATION

2-SEGMENTATION

1-IMAGE ADQUISICTION
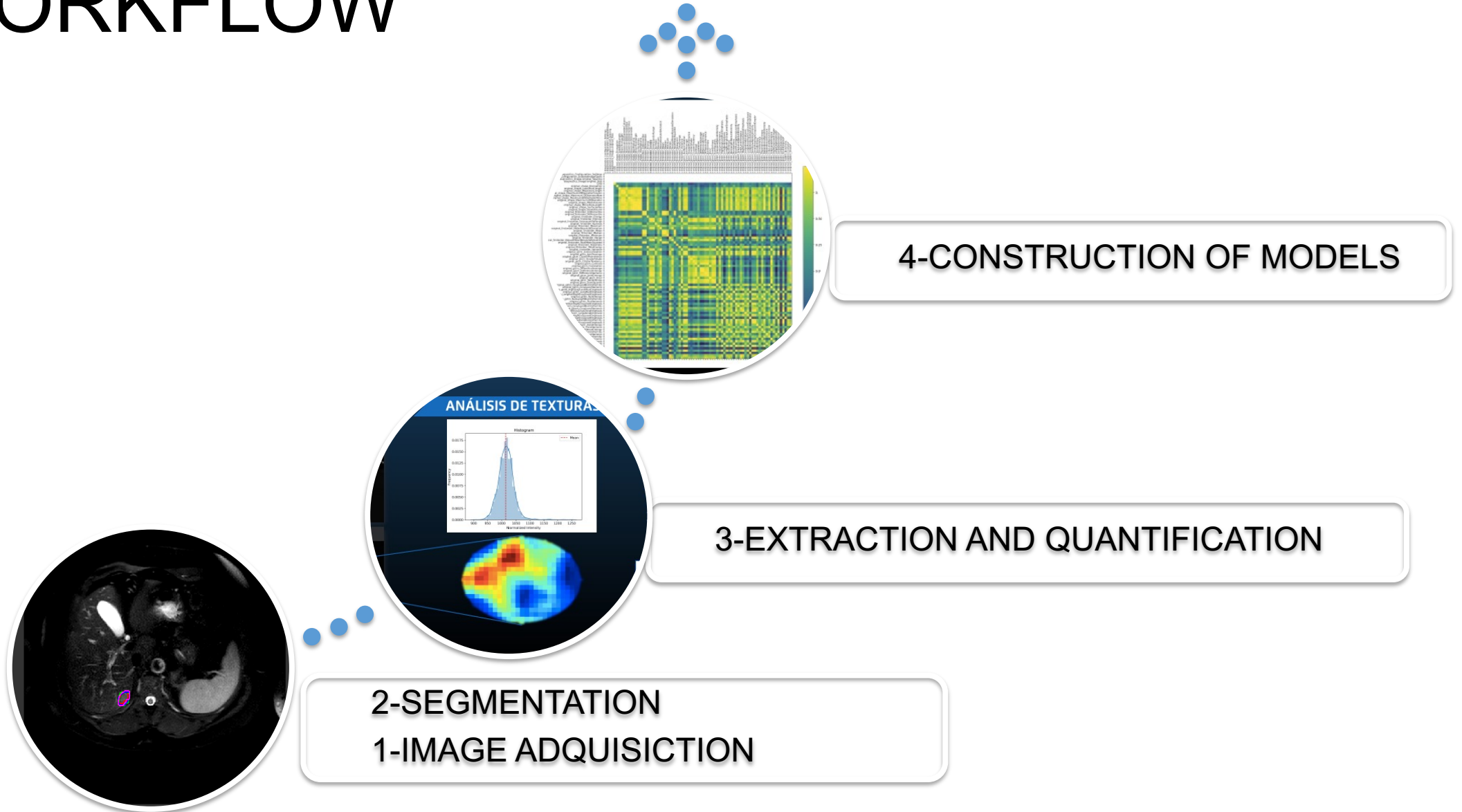
1. Image acquisition and reconstruction

- **Characteristics:** kV, mAs, slice size, breath control method, configuration, contrast.

- **Standardization of image data**

  - Can help to establish predictive models.

  - Important in the final results of the analysis (homogeneous criterion)

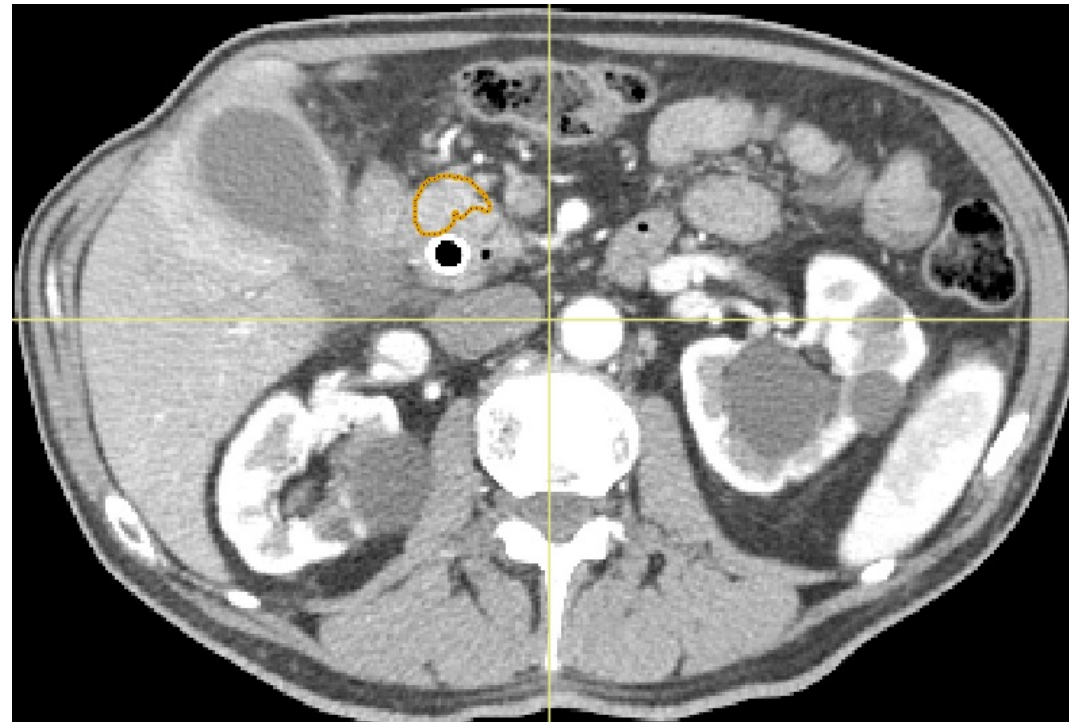Radiomics based on non-contrast CT images has shown in some studies a higher efficiency compared to contrast CT images.

Barat M, et al. Jpn J Radiol 2021;39:514–523.

2. Segmentation of the area of interest (I)

- ROI (Region of interest) = segmentation.

Types of segmentation: Manual, automatic, or semi-automatic.

- **Gold standard** → manual segmentation by experts but is operator dependent

- Automatic segmentation: uses preselected parameters and is ideal for its accuracy, reproducibility, and consistency but manual intervention is necessary to validate the automatic segmentation.

- There is no universal method, the same algorithm can give variable results.
- The semiautomatic segmentation is able to combine two previous procedures being the **most recommended**.

- Is crucial, **an error in this phase will modify the whole analisis.**

Weisberg EM, et al. Diagn Interv Imaging 2020;101:111–115.
Kaissis G, et al. Eur Radiol Exp 2019;3:41. Bartoli M, et al. Jpn J Radiol 2020;38:1111–1124

3. Extraction and quantification of features (I)

- **4 types of analysis:**

1. **Morphological**→ the most basic radiomics analysis

2. **Statistical**→ includes first-order (histogram) and highly-order features (texture)

3. **Regional**→ intratumor heterogeneity and characteristics around the tumor

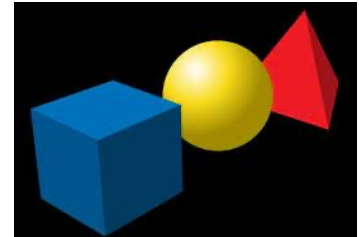4. **Model-based** → is analyzed with a mathematical approach

- **Morphological analysis includes:**

➢ **Shape**.

To evaluate physical characteristics and differentiates between malignant and benign lesions.

Include: diameter, volume, area under the curve (AUC), and wave.

Lesions are constructed in 3D images.

The most commonly used: **maximum and minimum diameter, and volume**.

Muhi A et al. J Magn Reson Imaging 2012;35:827–836. Zaheer A, et al. J Comput Assist Tomogr 2014;38:146–152. Cheng MF, et al. Sci Rep 2018;8:3651. Park S, et al. Diagn Interv Imaging 2020;101:555–564. Chu LC, etl al. AJR Am J Roentgenol 2019;213:349–357.

The volume is defined by counting the number of voxels in the tumor and multiplying by the volume of the voxel.

Volume is a **key parameter**, a short volume doubling time reflects high histological aggressiveness and suggests poor prognosis, volume is a tool for evaluating response to treatment.

Muhi A et al. J Magn Reson Imaging 2012;35:827–836. Zaheer A, et al. J Comput Assist Tomogr 2014;38:146–152. Cheng MF, et al. Sci Rep 2018;8:3651. Park S, et al. Diagn Interv Imaging 2020;101:555–564. Chu LC, etl al. AJR Am J Roentgenol 2019;213:349–357.

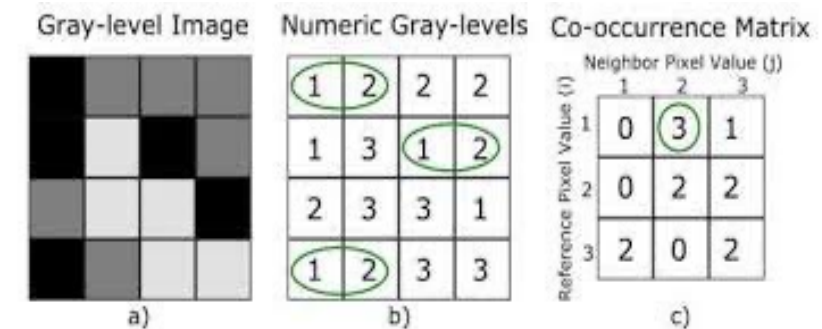# *3. Extraction and quantification of features (IV)*

➢ **Intensity**

- Is analyzed in histograms which are graphic representations of the intensity distribution in an image.

- Analysis **includes**:

- Range, mean, median, standard deviation (SD), minimum, maximum, kurtosis, energy, entropy (describes the randomness of the surrounding intensities within a grayscale image), uniformity, variance, and skewness

- Can be used to predict the nature of the lesion and prognosis.

- Characteristics are dependent on the reconstruction and image acquisition parameters (cut size and voxel size).

European Study Group on Cystic Tumours of the Pancreas. European evidence-based guidelines on pancreatic cystic neoplasms. Gut 2018;67:789–804.

3. Extraction and quantification of features (V)

➤ **Texture**

➤ Describes the relationship between neighboring pixels and their distribution through the nodes.

- Determines the **tumor's heterogeneity** (differentiation between benign and malignant lesions).

- For texture extraction, the most used method includes second-order statistics and co-occurrence matrix characteristics constructed using number, distance, and angle of gray levels in the image.

- **Includes:** correlation, clustering, contrast, energy, and entropy.

➢ **Wavelet**

- Allows to decompose the image data into different frequency components and uses these data to extract characteristics related to the **texture** and **intensity** of the image.

- These are filters that transform an array of complex lines or radio waves.

- The most common is the **Coiflet wave transformation**.

- They are used in the diagnosis and evaluation of response to treatment.

Zamboni F, et la. Transpl Int 2000;13:234–235.

- The relationship between the tumor and the surrounding healthy surface is another element of the tumor microenvironment.

- The discrete compaction is related to its circularity and this to the invasion around the tumor.

- The **neighboring gray tone matrix** is a parameter to differentiate gray tones, including busyness, complexity, and texture length.

- It is necessary to evaluate these data with statistical co-variance.

Sahani DV, et al. AJR Am J Roentgenol 2011;197:W53–W61. Kumar V, Gu Y, Basu S, Berglund A, Eschrich SA, Schabath MB, et al. Radiomics: the process and the challenges. Magn Reson Imaging 2012;30:1234–1248.
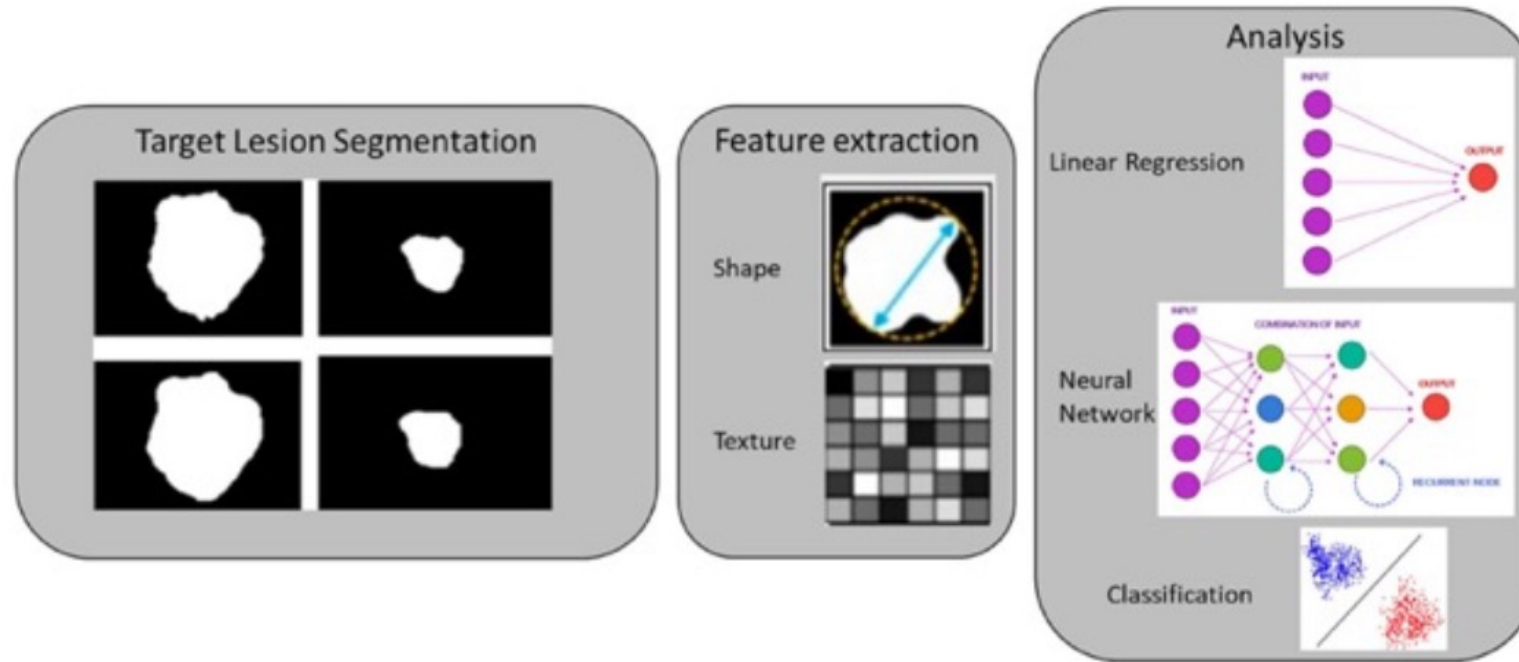
4. Construction of predictive models and prognosis in a non-invasive method

- Relationships between radiomics parameters and clinical variables.

- This can be done from direct statistical analysis based on hypotheses on machine learning methods.

Fig. 1 Radiomics flowdiagram

WHAT ARE THE APPLICATIONS?

Hallmarks of Cancer

Avoiding immune destruction

Tumor-promoting inflammation

Deregulating cellular energetics

Genome instability & mutation

Sustained proliferative signaling

Enabling replicative immortality

Evading growth suppressors

Resisting cell death

Inducing angiogenesis

Activating invasion and metastasis
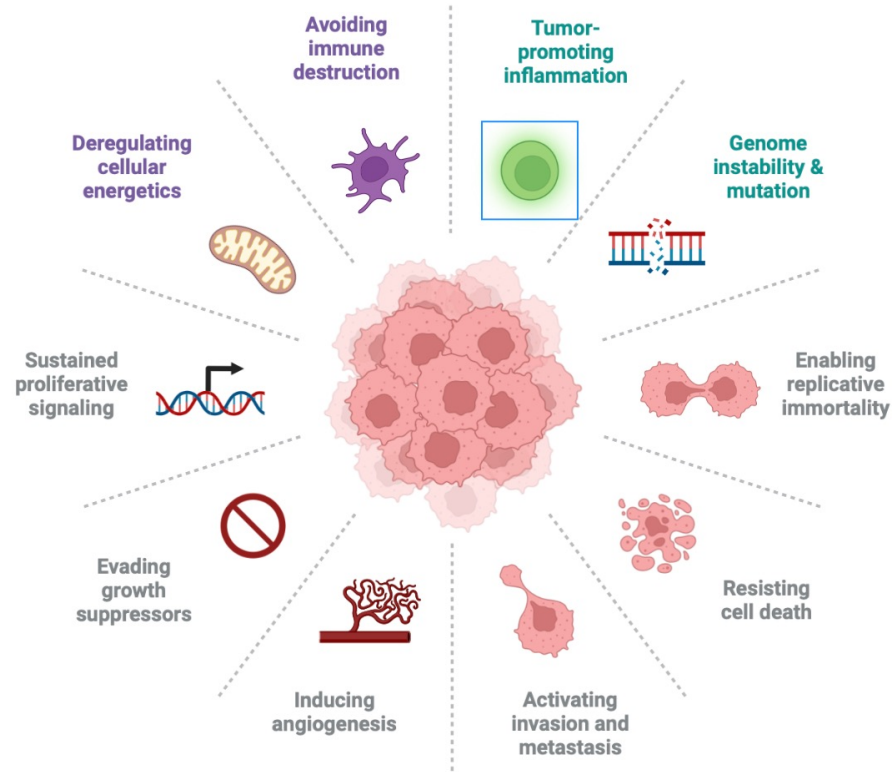
Differential diagnosis IN PANCREATIC LESIONS

Table 1
Radiomics studies in differentiation of pancreatic cystic lesions.

Studies	n	Type	Model	Clinical	Segmentation	Features	Differentation between entities
Dmitriev et al. [23]	134	IPMN ($n = 74$) MCN ($n = 14$) SCA ($n = 29$) SPN ($n = 17$)	Random forest classifier and convolutional neural networks (CNN)	Demographics	Semi-automated	Intensity, shape	84%
Wei et al. [24]	260	SCN, others	LASSO regression machine learning	Sex, location, moment of difference, mean rectangular fitting factor and size	Manual	Intensity texture	In the validation cohort ($n = 60$), sensitivity = 0.667, specificity = 0.818
Yang et al. [25]	53	MCN SCN	LASSO regression and random forest classifiers	Age, sex, location	Manual (two radiologist)	Texture	74% in 2 mm 83% in 5 mm
Hanania et al. [26]	53	IPMN	Logistic-regression model	Grade Fukuoka criteria	Manual (radiation oncology and radiologist)	360 radiomics features analyzed; 14 included in analysis	96%
Permuth et al. [27]	38	IPMN	Regression analysis	Age, sex, race, jaundice present, CA19-9, albumin, location, ductal communication, main duct dilation, size, solid component or mural nodule, high risk stigmata, worrisome features, 5 miRNA	Semi-automated	112 radiomics features analyzed; 14 included in analysis (texture, size and shape)	Combination 92%
Chakraborty et al. [28]	103	IPMN	Cox proportional hazards model	Age, size, solid component, pain, sex	Manual (radiologist)	12 intensity texture	80%, negative predictive value 94%

IPMN: intraductal papillary mucinous neoplasm, MCN: mucinous cystic neoplasm, SCA: serous cystadenoma of pancreas, SPN: solid pseudopapillary neoplasm, SCN: serous cystic neoplasm; LASSO: least absolute shrinkage and selection operator; CA19-9: carbohydrate antigen 19-9.

Differential diagnosis IN neuroendocrine tumors

Table 2
Radiomics studies in PNETs.

| Studies	n	Image	Features	Results
Lin et al. [30]	PNET ($n = 21$) Intra-pancreatic spleen ($n = 13$)	CT	Texture, entropy, skewness, kurtosis and uniformity	Less heterogeneous enhancement in arterial and portal phase in PNET (69% vs. 35%, $P = 0.06$; 100% vs. 29%, $P = 0.04$). Entropy and uniformity ($P < 0.01$). Uniformity with sensitivity of 85%-95% and specificity of 75%-83.3% to differentiate.
Choi et al. [31]	PNET ($n = 66$): grade 1($n = 45$); grade 2/3 ($n = 21$)	CT	Texture	Predictors of grade 2/3 were a well-defined margin (OR = 7.273). Low sphericity (OR = 0.409) in 2D arterial analysis, high skewness (OR = 1.972), low sphericity (OR = 0.408) in 3D analysis, low kurtosis (OR = 0.436), low sphericity in 2D portal (OR = 0.420) and in 3D (OR = 0.503) ($P < 0.05$), large surface area (OR = 2.007). Texture-based diagnosis was superior to CT findings (AUC = 0.774 vs. 0.683).
Canellas et al. [32]	Pre-surgery ($n = 101$)	CT	Texture	Size larger than 2 cm was predictive of higher grade (OR = 3.3; $P = 0.014$). Presence of vascular involvement (OR = 25.2; $P = 0.03$), pancreatic duct dilatation (OR = 6.0; $P = 0.002$), presence of lymphadenopathy (OR = 25.2; $P = 0.003$), entropy (OR = 3.7; $P = 0.008$) were predictive of more aggressive tumors. Differences were observed in progression free survival for grade 1 versus grade 2 tumors for PNETs with vascular involvement; and for tumors with entropy ($P < 0.001$).
Li et al. [33]	$n = 127$: pancreas adenocarcinoma ($n = 50$) PNETs ($n = 77$)	CT	Texture	Atypical PNETs had high mean, median, 5th, 10th and 25th percentiles ($P = 0.006, 0.024, < 0.001, 0.001, 0.021$, respectively) and low skewness ($P = 0.017$). No differences in 75th and 90th percentiles, kurtosis, and entropy between the two tumors.

PNET: pancreatic neuroendocrine tumor; CT: computed tomography; OR: odds ratio; AUC: area under curve.

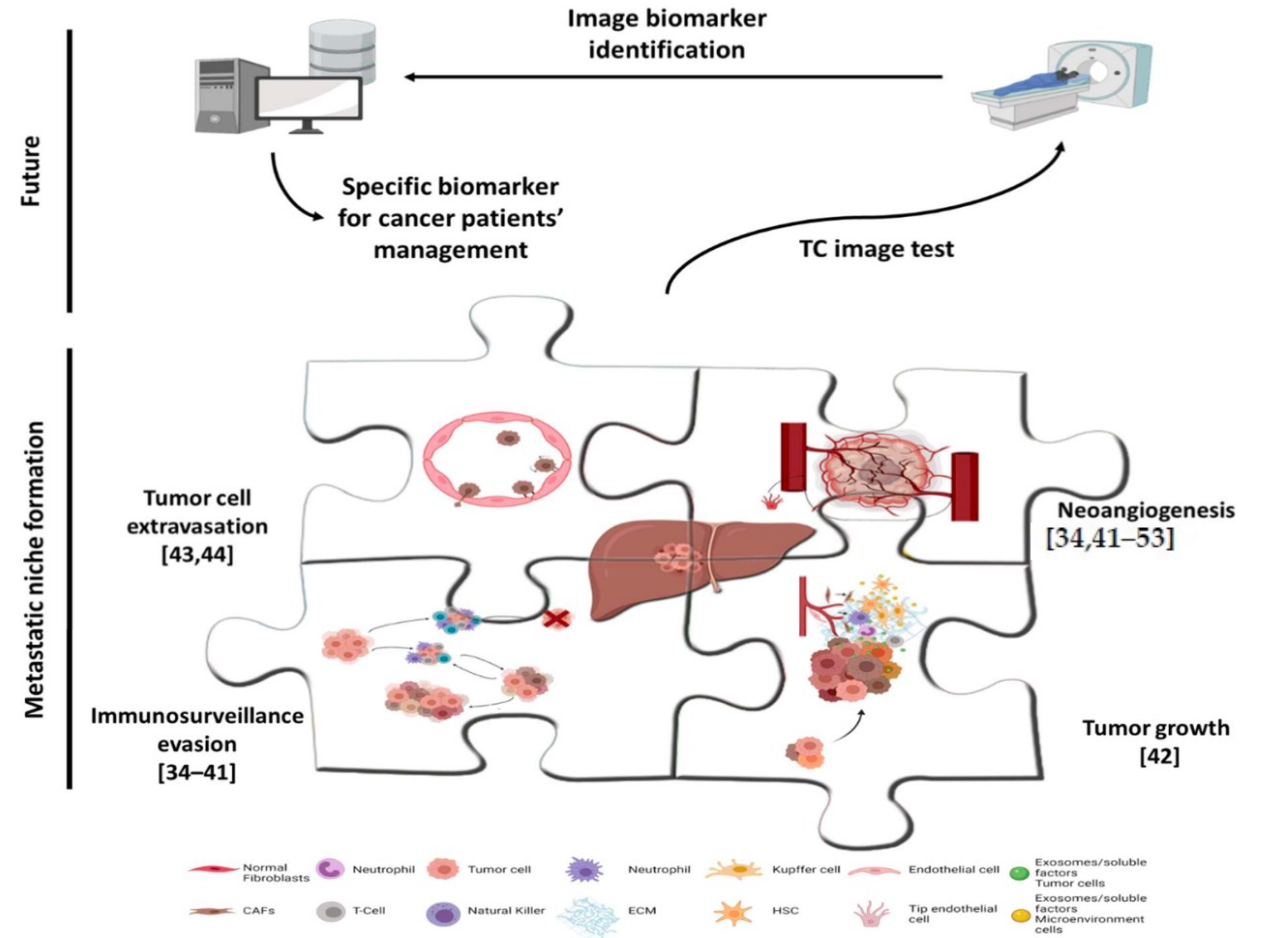# *PREDICTION: OVERALL SURVIVAL AND LOCAL CONTROL*

Lung
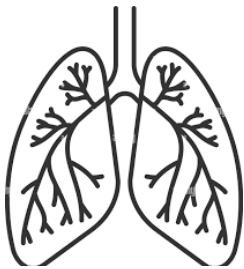
Table 1. Radiomics for prediction survival and local control.

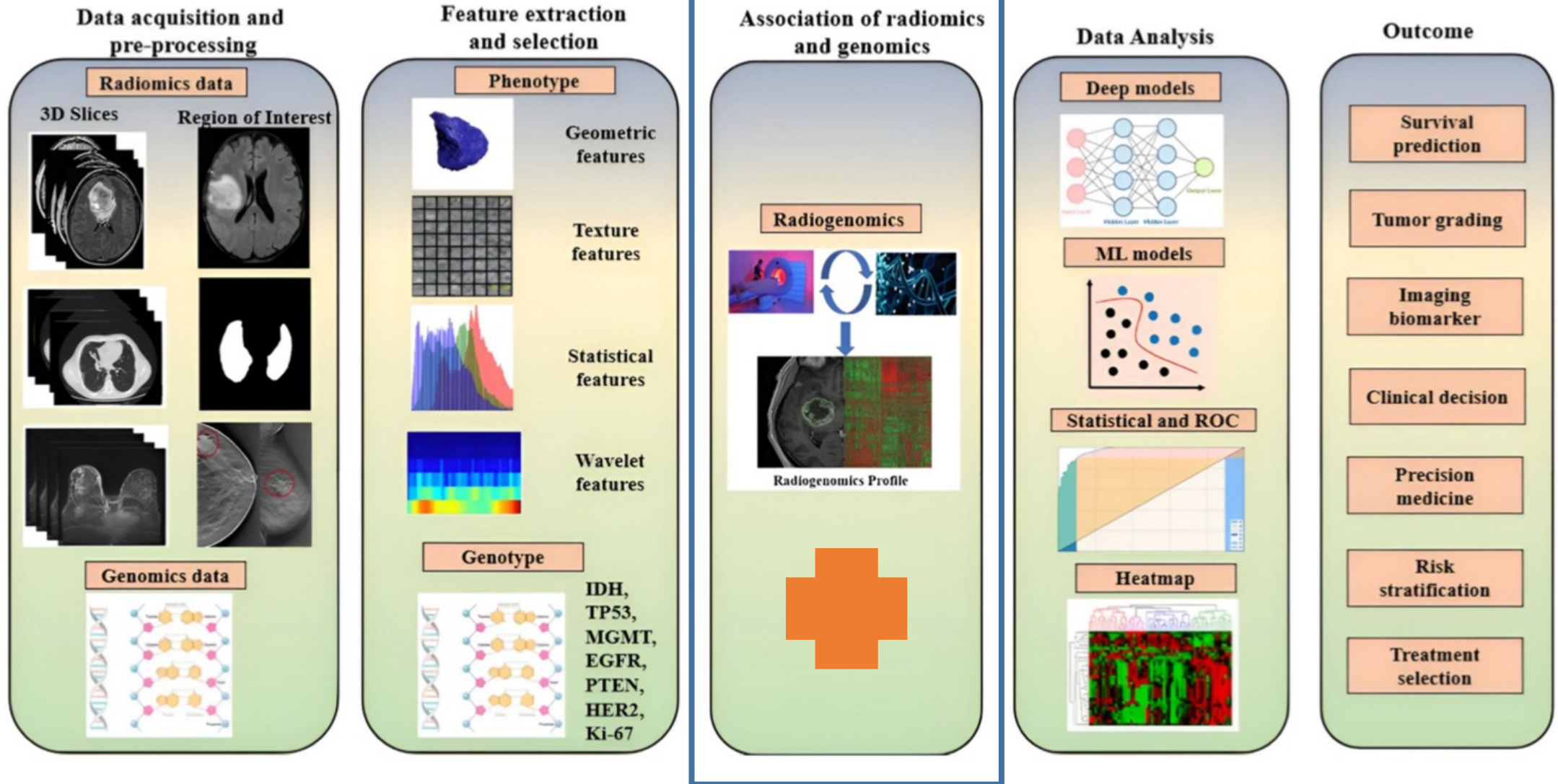| Study	n	Stage	Treatment	Image	Radiomic Features
Survival					
Huang[52]	282	I, II	-	CT	DFS: Texture
Parmar[23]	464	NSCLC	Pre-treatment	CT	OS: Size, intensity, shape, texture, wavelet
Coroller[61]	182	NSCLC	CRT	CT	DMFS: First order statistics, texture, wavelet
Song[51]	199	NSCLC	-	CT	OS: Wavelet
Fried[21]	91	III	RT	CT/PET	OS, LC, DMFS: Textura+clinical parameters
Ganeshan[22]		I-IV NSCLC	Pre-treatment	CT	OS: Texture
Depeursinge[54]	101	I, AC, resected	Surgery	CT	DFS: Texture
Grove[49]	108	Early	-	CT	OS: Shape, texture
Balagurunathan[62]	59	NSCLC	-	CT	OS: Shape, texture
Carvalho[63]	220	I-IIIB	CRT	PET	OS: Delta radiomics (volume, texture and intensity-volume histogram)
Li[64]	92	I-IIA	SBRT	CT	OS: Morphology and clinical parameters
Aerts[19]	647		CRT	CT	OS: Shape, intensity, texture
Song[65]	152	I-IV	TKI	CT	OS: Wavelet
Huynh[39]	113	I, II	SBRT	CT	OS: First order statistics, texture, shape Metastases: Wavelet
Local control					
Mattonen[40]	45	Recurrence	SBRT	CT	Texture
Pyka[48]	45	I-IIA	SBRT	PET	Entropy
Lovinfosse[66]	63	I-II	SBRT	PET	Texture
Wu[67]	101	I	SBRT	PET	Radiomics and histology
Cook[20]	53	IB-III	CRT	PET	Coarseness, contrast, busyness
Kang[55]	116	III	CRT	PET	SUVmax, AUC-CSH
Vaidya[68]	27	IV	SBRT	CT/PET	IVH in PET, COV in CT

CT: computed tomography; DFS: disease free survival; NSCLC: non-small cell lung cancer; CRT: chemoradiotherapy, OS: overall survival; RT: radiotherapy; PET: positron emission tomography; LC: local control; DMFS: distant metastases free survival; AC: adenocarcinoma; SBRT: stereotactic body radiotherapy; TKI: tirosin kinasa inhibitors; SUV: standardized uptake value; AUC-CSH: area under curve of the cumulative SUV-volume histogram; IVH: intensity volume histogram ; COV: coefficient of variation

Radiogenomics

- The genetic study of tumors has allowed the development of **targeted therapies**, and the **stratification** of patients in terms of risk of relapse, prognosis, prediction of response and survival.

- The correlation of genetic alterations or tumor microenvironment and radiological findings allows the use of these **imaging tests** as a non-invasive tool for personalized medicine.

de la Pinta C, Castillo ME, Collado M, Galindo-Pumariño C, Peña C. Radiogenomics: Hunting Down Liver Metastasis in Colorectal Cancer Patients. Cancers (Basel). 2021 Nov 5;13(21):5547.

LIVER METASTASES

Table 1. Clinical benefits of radiomic and radiogenomics in CRC liver metastatic patients.

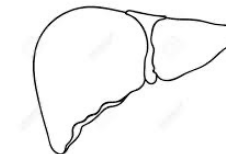| Study	Design	Imaging Modalities	Sample Size	Study Cohorts and Validation	Tools for Radiomics Calculations	Statistical Model Construction
			Early diagnosis of colorectal cancer metastasis			
Becker et al., 2018 [5]	Preclinical	MRI	8 male mice	One cohort	MATLAB routine	Linear regression model, Pearson correlation test and hierarchical cluster analysis
Taghavi et al., 2021 [6]	Retrospective	CT	91 CRC without LM at diagnosis	Two cohorts. Patients with metastases in follow-up of ≥24 months ($n = 67$); and patients who developed metachronous liver metastases <24 months ($n = 24$). No validation	Philips Intellispace Portal software and PyRadiomics	Kruskal–Wallis test, inter-correlated features and Bayesian-optimized random forest was used for prediction models.
Rao et al., 2014 [7]	Retrospective	CT	29 CRC patients	Three cohorts. Patients without LM ($n = 15$), with synchronous LM ($n = 10$) and metachronous LM within 18 months following primary staging ($n = 4$). No validation	MATLAB routine	Student's t test or Mann–Whitney U test. ROC analyses to determine the potential diagnostic performance of the respective texture parameters for diagnosing the presence of metastatic disease.
Liang et al., 2019 [8]	Retrospective	MRI	108 rectal cancer patients	Two cohorts. 54 patients with LM and 54 without LM. The results of the one-round cross-validation were stabilized and representative.	Python in Anaconda3 platform with Scikit-learn and Matplotlib packages.	Models were evaluated with indicators of accuracy, sensitivity, specificity and AUC, and compared by DeLong test.
Oyama et al., 2019 [9]	Retrospective	MRI	150 liver tumors. 50 HCC, 50 LM and 50 HHs in 37, 23 and 33 patients	One cohort.	MATLAB Image Processing Toolbox, Signal Processing Toolbox, Statistics and Machine Learning Toolbox, and Wavelet Toolbox	Two machine learning models: a logistic classifier model with an elastic net penalty and extreme gradient boosting (XGBoost)
Li et al., 2017 [10]	Retrospective	MRI	162 patients	Three cohorts. HHs ($n = 55$), LM ($n = 67$) and HCC ($n = 40$). The test datasets validated the reliability of the models	R software (R Core Team, Vienna, Austria) and MATLAB R2013b (Mathworks, Natick, MA, USA)	Kruskal–Walls test, ROC curve and AUC analysis to differentiate three subtypes. K-nearest neighbor classifier model, back-propagation artificial neural network classifier model, support vector machine and logistic regression were used for improving accuracy for classifier.

de la Pinta C, Castillo ME, Collado M, Galindo-Pumariño C, Peña C. Radiogenomics: Hunting Down Liver Metastasis in Colorectal Cancer Patients. Cancers (Basel). 2021 Nov 5;13(21):5547.

Table 1. *Cont.*

Study	Design	Imaging Modalities	Sample Size	Study Cohorts and Validation	Tools for Radiomics Calculations	Statistical Model Construction
Rahmim et al., 2019 [25]	Retrospective	FDG PET/CT	52 CRLM patients	One cohort	Hermes Hybrid Viewer PDR and MATLAB	Kaplan–Meier and Cox proportional hazards models
Dercle et al., 2020 [26]	Retrospective	CT	667 CRLM patients	Two cohorts. Randomly assigned (2:1) to training or validation sets. Predicted tumor sensitivity to treatment was measured using AUC in the validation sets of the four cohorts consisting of patients that were not used for training.	MATLAB (Mathworks, Natick, MA, USA)	Variance and v2 test were performed to compare categorical variables. Cox regression was used to investigate the effect of survival variables, and log-rank test was used to compare survival times of two groups.
Dohan et al., 2019 [27]	Multicenter prospective	CT	491 CRLM patients treated by FOLFIRI and bevacizumab	Two cohorts. Training cohort in 120 patients, and validate cohort in 110 patients. External validation was performed in another cohort of 40 patients	TexRAD Ltd., (Somerset, UK)	Multivariable Cox, Kaplan–Meier and log-rank
Ravanelli et al., 2019 [28]	Retrospective	CT	43 CRLM patients	Two cohorts. 23 treated with bevacizumab-containing chemotherapy (group A), and 20 with standard chemotherapy (group B)	MATLAB (Natick, MA, USA)	Multivariable logistic regression

CT: computed tomography; MRI: magnetic resonance imaging; FDG PET/CT: fluorodeoxyglucose positron emission tomography/computed tomography; CRC: colorectal carcinoma; LM: liver metastases; CRCLM: colorectal carcinoma liver metastases; HCC: hepatocellular carcinoma; HHs: hepatic hemangiomas; FLLs: focal liver lesions; AUC: area under curve; ROC: receiver operating characteristic.

PROSTATE CANCER

Table 4. Overview of radiogenomic literature on prostate cancer.

Reference	Molecule Studied	Imaging Performed	Results	Approach	Method
McCann et al. [124]	PTEN	MRI	Perfusion imaging contrast uptake, T2-weighted signal-intensity skewness	Classical	Radiomic
Stoyanova et al. [158]	General gene expression	MRI	Radiomic signatures	Classical	Radiomic
Renard-Penna et al. [119]	RNA expression signature derived from cell cycle proliferation genes (Prolaris®)	mpMRI	Correlation with Gleason score (r = 0.199, p = 0.04) and PIRADS sum score (r = 0.26, p = 0.007)	Classical	Radiomic
Jamshidi et al. [125]	Whole-exosome DNA sequencing	mpMRI	No statistically significant linear correlation between individual mutations and mpMRI imaging parameters or PIRADS scores (p = 0.3)	Classical	Radiomic
Houlahan et al. [130]	Small nucleolar RNAs	mpMRI	Elevated snoRNA abundance may be a novel hallmark of nimbotic tumors (AUC: 0.87; 95%CI: 0.75–0.99)	Classical	Radiomic
Li P et al. [159]	Differentially expressed genes	MRI	MRI visibility (AUC: 0.86), progression-free survival HR = 2.53 (1.55–4.11), p < 0.001 BCR-free survival HR = 1.3 (1.04–1.63), p = 0.021	Classical	Radiomic
Eineluoto et al. [160]	PTEN and ERG	MRI	MRI-invisible lesions had less PTEN loss and ERG-positive expression compared with patients with MRI-visible lesions (17.2% vs. 43.3%, p = 0.006; 8.6% vs. 20.0%, p = 0.125)	Classical	Radiomic
Hectors et al. [161]	40 gene expression signatures plus Decipher®	MRI	Prediction of Gleason score of 8 or greater (AUC 0.72) and prediction of a Decipher® score of 0.6 or greater (AUC 0.84).	Classical	Radiomic
Li L et al. [162]	Decipher®	MRI	Model outperformed the prediction using PIRADS v2 (AUC = 0.67), and comparable performance with Gleason grade group (AUC = 0.80)	Classical	Radiomic
Sun et al. [163]	Full transcriptome genetic profiles	mpMRI	Weak association of mpMRI features and hypoxia gene expression (p < 0.05).	Classical	Radiomic
Fischer et al. [27]	Gene and miRNA expression (Alanyl membrane aminopeptidase, microRNA-mir-217, mir-592, mir-6715b)	mpMRI	T2c and T3b prostate cancer stages being highly correlated with aggressiveness on related imaging features (average r = ± 0.75)	Classical	Radiomic
Wibmer et al. [150]	Prolaris® test	MRI	ECE on MRI had significantly higher mean cell cycle risk score (reader 1: 3.9 vs. 3.2, p = 0.015; reader 2: 3.6 vs. 3.2, p = 0.045)	Classical	Radiomic
Vander-Weele et al. [164]	PTEN	mpMRI	Imaging uptake parameters showing mathematical correlation with PTEN expression (r = 0.25, p < 0.1 and r = 0.43, p < 0.01), and T2w unevenness also showed some correlation tendency (r = −0.25, p < 0.1)	Classical	Radiomic
Switlyk et al. [165]	PTEN	MRI	ADC was negatively correlated with Gleason score (p = 0.001) and tumor size (p = 0.023)	Classical	Radiomic

ADC = apparent diffusion coefficient; AUC = area under the curve; DNA = deoxyribonucleic acid; ECE = extracapsular extension; ERG = ETS-related gene; mpMRI = multiparametric magnetic resonance imaging; miRNA = micro ribonucleic acid; PIRADS = prostate imaging reporting and data system; PTEN = phosphatase and tensin homolog; T2w = T2-weighted.
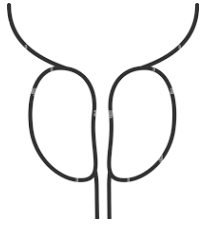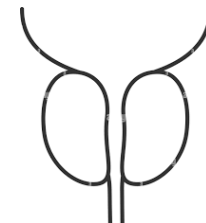
Ferro M, et al. Prostate Cancer Radiogenomics-From Imaging to Molecular Characterization. Int J Mol Sci. 2021 Sep 15;22(18):9971

Table 3. Compilations of studies on the association of imaging and genomics.

| Biomarker	Description	Test Source	Analysis	Study	Results
Prostate cancer antigen 3	Prostate-specific mRNA quantification	Prostate biopsy	Negative prior biopsy	De Luca et al. [138]	Significant association between PCA3 score and PI-RADS grade groups 3, 4, and 5 ($p = 0.006$)
			Two negative prostate biopsies	Alkasab et al. [139]	PCA3 not statistically correlated with PCa diagnosis ($p = 0.128$) and PCA3 associated with high-grade PCa at final pathology ($p = 0.0435$)
			No prior biopsy	Fernstermaker et al. [140]	PCA3 associated with MRI suspicion score of 2 and 3 ($p = 0.004$), not 4 and 5 ($p = 0.340$)
			Negative prior biopsy	Perlis et al. [141]	Normal PCA3 score gave a negative predictive value of 100% ($p < 0.0001$)
Decipher test®	22 RNA markers for prognosis and prediction of metastasis	RP or prostate biopsy	Low and intermediate PCa	Martin et al. [142]	Decipher® biopsy genomic test was associated with Gleason grade group and it was independent of PIRADSv2 score
			Defining the favorable intermediate-risk prostate cancer	Falagario et al. [143]	Unfavorable intermediate-risk category ($p < 0.001$) and Decipher® test ($p = 0.012$) were statistically significant predictors of adverse pathology; mpMRI did not maintain statistical significance ($p = 0.059$)
			Prediction of BCR	Jambor et al. [144]	Decipher® genomic score and mpMRI could not improve predictive performance of biochemical recurrence compared with the individual use of these features
			mpMRI could predict aggressive prostate cancer features	Beksac et al. [145]	Association of Decipher® score was significantly with lesion size ($p = 0.03$), PIRADS score ($p = 0.02$) and extraprostatic extension ($p = 0.01$)
			Correlation between MRI phenotypes of PCa as defined by PI-RADS v2 and Decipher	Purysko et al. [146]	MRI-visible lesions had higher Decipher® scores than MRI-invisible lesions ($p < 0.0001$); some lesions classified as intermediate/high risk by Decipher® are invisible on MRI
			BCR and adverse pathology prediction	Li et al. [45]	New imaging-based nomogram; AUC (0.71, 95% CI 0.62–0.81) better than Decipher® AUC (0.66, 95% CI 0.56–0.77) and prostate cancer risk assessment (CAPRA) score AUC (0.69, 95% CI 0.59–0.79)

Table 3. *Cont.*

Biomarker	Description	Test Source	Analysis	Study	Results
Oncotype Dx test®	5 reference genes and 12 cancer genes generating a genomic prostate score (GPS)	Prostate biopsy	Association between mpMRI and Oncotype Dx test®GPS	Leapman et al. [147]	GPS differences among MRI categories for patients with Gleason pattern 3 + 4 ($p = 0.010$), not in Gleason pattern 3 + 3
			GPS to predict adverse pathology	Salmasi et al. [148]	GPS is a significant predictor for adverse pathology ($p < 0.001$)
ConfirmMDx®	Alterations in DNA methylation	Prior negative biopsies	mpMRI PIRADS score lesions after ConfirmMDx® sampling	Artenstein et al. [149]	Negative ConfirmMDx® test is in accordance with negative MRI results (71.4%). ConfirmMDx® sampling may be useful as a fusion-targeted biopsy rather than systematic biopsy
Prolaris test®	46-mRNA genomic test	Prostate biopsy	Associations between MRI and the expression levels of cell cycle genes	Wibmer et al. [150]	In the RP subgroup, ECE on MRI ($p \leq 0.001$–0.001) and cycle genes risk scores ($p = 0.049$) were significantly associated with Gleason score 4 + 3 or higher, ECE and lymph node metastases

AUC = area under the curve; BCR = biochemical recurrence; DNA = deoxyribonucleic acid; ECE = extracapsular extension; GPS = genomic prostate score; mpMRI = multiparametric magnetic resonance imaging; mRNA = micro ribonucleic acid; PCA3 = prostate cancer antigen 3; PIRADS v2 = prostate imaging reporting and data system version 2; RP = radical prostatectomy.

RENAL CELL CARCINOMA
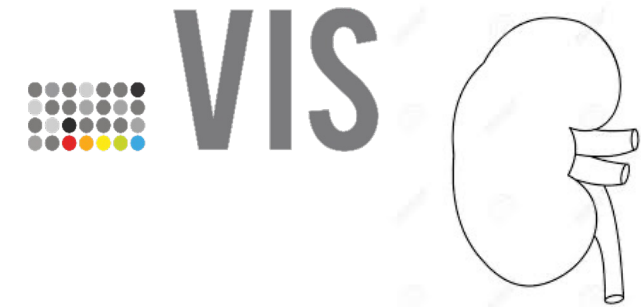
Table 1. Summary of 20 reviewed articles on radiogenomics in clear cell renal cell carcinoma. Nature of feature extraction is indicated by "Radiologist" if features are scored by one or more radiologists. Elsewise, software derived features are indicated by "Computational". Number of selected features indicated in parenthesis. TAT (total adipose tissue), VAT (visceral adipose tissue), AUC (area under the curve), OR (odds ratio), HR (hazard ratio), CSS (cancer specific survival), OS (overall survival), PFS (progression free survival).

Author	Title	Year of Publication	Patient #	Feature Extraction (Number)	±Machine Learning	Image Phase Used	Genes Studied	Outcome
Karlo et al. [9]	Radiogenomics of Clear Cell Renal Cell Carcinoma: Associations between CT Imaging Features and Mutations	2014	233	Radiologist (10)	–	CT	BAP1 VHL KD5MC	BAP1 and KD5MC: renal vein invasion (OR 3.50 and 3.89) VHL: ill-defined margin (OR 0.49), nodular enhancement (OR 2.33), intratumoral vasculature (OR 0.51)
Shinagare et al. [10]	Radiogenomics of clear cell renal cell carcinoma: Preliminary findings of the cancer genome atlas–renal cell carcinoma (TCGA–RCC) imaging research group	2015	103	Radiologist (6)	–	Contrast-enhanced CT	BAP1 MUC-4	BAP1: Ill-defined margin and calcification MUC4: Exophytic growth
Greco et al. [11]	Relationship between visceral adipose tissue and genetic mutations (VHL and KDM5C) in clear cell renal cell carcinoma	2021	97	Computational (3)	–	CT	KDM5C vs. VHL	KDM5C higher TAT and VAT area than VHL
Feng et al. [12]	Identifying BAP1 Mutations in Clear-Cell Renal Cell Carcinoma by CT Radiomics: Preliminary Findings	2020	54	Computational (58)	+ (Random Forest)	CT	BAP1	AUC 0.77
Kocak et al. [13]	Machine learning-based unenhanced CT texture analysis for predicting BAP1 mutation status of clear cell renal cell carcinomas	2020	65	Computational (6)	+ (Random Forest)	CT	BAP1	AUC 0.897

Gopal N, et al. The Next Paradigm Shift in the Management of Clear Cell Renal Cancer: Radiogenomics-Definition, Current Advances, and Future Directions. Cancers (Basel). 2022 Feb 4;14(3):793.

Assessment of response to treatment

- The correct assessment of response in the treatment is fundamental in defining the success or failure of treatment interventions.

- Prediction of early response would improve treatment selection in these patients.

  - Radiomics and radiogenomics could be very useful.

Technical problems, limitations and challenges (I)

- CT acquisition

- Reconstruction

- Kernels

- Tube currents

- Slice size

- Voxel size

- Grey level

- Delay of contrast enhancement

Technical problems, limitations and challenges (II)

- Standardization of protocols is therefore important in **clinical applications**

- Also many of the comparisons between diagnostic entities using radiomics are subjective and not clinically applicable.

Mayerhoefer ME, et al. Med Phys 2009;36:1236–1243.
Varghese BA, et al. AJR Am J Roentgenol 2019;212:520–528.

CONCLUSIONS

- Radiomics is a promising non-invasive tool for the diagnosis and clinical management of tumors and the patients.

- The usefulness of radiomics has been studied in the differential diagnosis of benign, premalignant and malignant lesions.

- In addition, it can help in the more precise definition of lesions for chemotherpay and radiotherapy and assessment of response.

- Radiomics provides a more adequate and reproducible measurement of the tumor than other methods.

- In addition, the combination of radiomics and genomics has a promising future to biomarkers.

- However, image acquisition protocols and radiomic analysis systems need to be standardized and validation cohorts are needed.

- Further studies are needed to consolidate the available data.

THANK YOU